RENAL FAILURE
2024, VOL. 46, NO. 2, 2375033
https://doi.org/10.1080/0886022X.2024.2375033

Taylor & Francis
Taylor & Francis Group

CLINICAL STUDY

OPEN ACCESS Check for updates

Screening of active components in *Astragalus mongholicus Bunge* and *Panax notoginseng* formula for anti-fibrosis in CKD: nobiletin inhibits Lgals1/PI3K/AKT signaling to improve renal fibrosis

Fang Yang[a,b,c#], Tong Li[b#], Xiao-qian Zhang[a,b], Yi Gong[a,b], Hongwei Su[d], Junming Fan[e], Li Wang[b], Qiong-dan Hu[a,b] and Rui-zhi Tan[b]

[a]Department of Nephrology, the Affiliated Traditional Chinese Medicine Hospital, Southwest Medical University, Luzhou, China; [b]Research Center of Integrated Traditional Chinese and Western Medicine, the Affiliated Traditional Chinese Medicine Hospital, Southwest Medical University, Luzhou, China; [c]Department of Nephrology, Sichuan Integrative Medicine Hospital, Chengdu, China; [d]Department of Urology, the Affiliated Traditional Chinese Medicine Hospital, Southwest Medical University, Luzhou, China; [e]Department of Nephrology, the First Affiliated Hospital of Chengdu Medical College, Chengdu, China

ABSTRACT

The *Astragalus mongholicus Bunge* and *Panax notoginseng* formula (A&P) has been clinically shown to effectively slow down the progression of chronic kidney disease (CKD) and has demonstrated significant anti-fibrosis effects in experimental CKD model. However, the specific active ingredients and underlying mechanism are still unclear. The active ingredients of A&P were analyzed by Ultra-high performance liquid chromatography-tandem mass spectrometry (UPLC-HR-MS). A mouse model of CKD was constructed by 5/6 nephrectomy. Renal function was assessed by creatinine and urea nitrogen. Real-time PCR and Western Blot were performed to detect the mRNA and protein changes in kidney and cells. An *in vitro* fibrotic cell model was constructed by TGF-β induction in TCMK-1 cells. The results showed that thirteen active ingredients of A&P were identified by UPLC-HR-MS, nine of which were identified by analysis with standards, among which the relative percentage of NOB was high. We found that NOB treatment significantly improved renal function, pathological damage and reduced the expression level of fibrotic factors in CKD mice. The results also demonstrated that Lgals1 was overexpressed in the interstitial kidney of CKD mice, and NOB treatment significantly reduced its expression level, while inhibiting PI3K and AKT phosphorylation. Interestingly, overexpression of Lgals1 significantly increased fibrosis in TCMK1 cells and upregulated the activity of PI3K and AKT, which were strongly inhibited by NOB treatment. NOB is one of the main active components of A&P. The molecular mechanism by which NOB ameliorates renal fibrosis in CKD may be through the inhibition of Lgals1/PI3K/AKT signaling pathway.

ARTICLE HISTORY
Received 20 March 2024
Revised 14 June 2024
Accepted 26 June 2024

KEYWORDS
Nobiletin; renal fibrosis; Lgals1; PI3K/AKT; chronic kidney disease

Introduction

Chronic kidney disease (CKD) poses a significant global public health challenge. According to 2019 data, the prevalence of CKD in China is 8.2%, corresponding to approximately 82 million cases. Alarmingly, CKD directly claims the lives of 1.2 million patients worldwide each year, with more than 170,000 deaths occurring in China alone[1]. Renal fibrosis, a common pathology associated with CKD, greatly hastens the progression toward end-stage kidney disease (ESKD), a condition with a notably high mortality rate [2]. However, the improvement of renal fibrosis remains a formidable obstacle, necessitating the quest for effective treatment.

Traditional Chinese Medicine (TCM) has gained recognition from the World Health Organization as a viable option for treating chronic diseases [3]. According to our previous studies, a clinical study involving 120 non-dialysis patients with CKD demonstrated the efficacy of *Astragalus mongholicus Bunge* and *Panax notoginseng* formula (A&P) in slowing the decline of kidney function in individuals with stage 3-5 CKD [4]. Another clinical study involving 60 patients with primary Nephrotic Syndrome (NS) showed that the addition of A&P adjuvant therapy to hormone and cyclophosphamide resulted in more effective improvement of NS patients' hypercoagulable state, immune regulation, and reduction in complications such as thrombosis, embolism, and infection,

CONTACT Qiong-dan Hu huqiongdan@swmu.edu.cn; Rui-zhi Tan tanruizhi627@swmu.edu.cn 182# chunhui road, Luzhou, Sichuan 646000, China.
[#]These authors contributed equally to this work.

Supplemental data for this article can be accessed online at https://doi.org/10.1080/0886022X.2024.2375033.

ultimately improving patient prognosis [5]. Previous research has also indicated that A&P may inhibit macrophage inflammation mediated by Mincle, alleviate cisplatin-induced acute kidney injury (AKI), and improve kidney injury in diabetic nephropathy by either inhibiting apoptosis or promoting autophagy [6, 7]. Therefore, the significant clinical efficacy and molecular mechanisms of A&P in improving renal function are partially demonstrated. However, due to the complex composition of A&P and its diverse compounds, its efficacy and mechanisms of action have remained challenging to ascertain. Therefore, the objective of this study was to employ ultra-high performance liquid chromatography-tandem mass spectrometry (UPLC-HR-MS) to identify the active ingredients of A&P and investigate the molecular mechanism of Nobiletin (NOB), the primary active ingredient in A&P, in ameliorating renal fibrosis in CKD.

Nobiletin, a naturally occurring dietary polyoxymethylated flavonoid, possesses a wide range of beneficial properties, including antioxidant effects, antitumor activity, immunomodulation, neuroprotection, improvement of abnormal coronary lipid metabolism, blood glucose reduction, and fibrosis amelioration [8]. It has been identified as a promising phytochemical within the citrus flavonoid family, particularly for its potential in preventing and treating chronic diseases [9]. These flavonoids have demonstrated effectiveness in reducing oxidative stress, improving glucose tolerance, enhancing insulin sensitivity, suppressing inflammation, addressing lipid metabolism disorders, regulating adipocyte differentiation and apoptosis, and improving endothelial cell function [10–14]. Nobiletin has been found to decrease the expression of transforming growth factor-beta (TGF-β), connective tissue growth factor, fibronectin, and collagen, thus improving cardiac fibrosis [15]. Furthermore, recent studies have shown that pretreatment with Nobiletin can mitigate kidney injury caused by renal ischemia-reperfusion through the PI3K/AKT pathway by inhibiting reactive oxygen species production and apoptosis [16, 17]. Additionally, Nobiletin has demonstrated the ability to attenuate renal fibrosis and epithelial-mesenchymal transition (EMT), alleviate oxidative stress and iron-related injury, and delay chronic kidney disease progression in mice with unilateral ureteral obstruction [18]. Moreover, Nobiletin has been recognized as a potential therapeutic agent for drug-drug interactions and has been shown to protect the kidneys from methotrexate-induced nephrotoxicity by modulating metabolism [19]. Therefore, further comprehensive investigation is urgently needed to determine the therapeutic potential of Nobiletin as an ingestible botanical natural compound for effectively improving renal fibrosis in chronic kidney disease.

Galectin-1 (Gal-1), encoded by lectin, galactoside-binding, soluble (Lgals) 1, is a member of the Galectin family that interacts with β-galactoside residues of cell surface and matrix glycoproteins through the carbohydrate recognition region and can form peptide-peptide binding through the N-segment region [20, 21]. Gal-1 has recently emerged as a novel fibrotic protein in type 1 and type 2 diabetes, playing a crucial role in the development of liver, kidney, pancreatic, and lung fibrosis and serving as a key mediator between tissue repair and fibrosis [21, 22]. It is found in the cytoplasm and cell membranes of certain fibroblasts, immune cells, and thickened endothelial cells along the dermis. Gal-1 interacts with extracellular matrix (ECM) molecules produced by fibroblasts and immune cells, influencing fibroblast morphology, adhesion, proliferation, and migration on the cell surface. These interactions lead to the formation of supramolecular structures in the extracellular space, contributing to the pathological inflammatory response observed in keloids [23]. In cases of persistent inflammation, Gal-1 becomes consistently upregulated, thereby promoting keloid formation through activation of the PI3K/AKT signaling pathway [22]. Increased expression of Lgals1, in turn, enhances the phosphorylation of AKT, mTOR, and P70 kinase, potentially amplifying Lgals1 transcription in a positive feedback loop [21, 24, 25]. Moreover, recent research has highlighted the significance of non-coding RNAs in regulating key regulators of myofibroblast differentiation and ECM production, with the PI3K/Akt signaling pathway being a major regulatory pathway [26]. In a previous study utilizing weighted gene co-expression network analysis (WGCNA) to investigate the transition from acute kidney injury (AKI) to CKD, we identified pIp1 and Lgals1 as pivotal genes in post-AKI renal fibrosis [27]. However, there is still a lack of evidence whether Lgals1 is a key gene in the progression of CKD and whether it is involved in regulating the PI3K/AKT signaling pathway leading to renal fibrosis.

Therefore, we identified Nobiletin as the active ingredient of A&P by UPLC-HR-MS. To further validate the pharmacodynamic mechanism of Nobiletin, we explored the potential therapeutic effect and molecular mechanism of Nobiletin in improving renal fibrosis in chronic kidney disease by establishing 5/6 nephrectomy mice *in vivo* and TGF-β stimulated TCMK-1 cell *in vitro*.

Materials and methods

Preparation of A&P and NOB for UPLC-HR-MS

The main components of A&P reagent consist of 3 g of *Astragalus propinquus Schischkin*, 1 g of *Panax notoginseng*, 3 g of *Achyranthes bidentata*, 3 g of *Ecklonia kurome*, and 3 g of *Angelica sinensis*, all of which were obtained from TCM Hospital Affiliated to Southwest Medical University in Luzhou, Sichuan, China. Standard compounds for HPLC quality control analysis, including (-)-Epigallocatechin, Puerarin, Glycitin, Notoginsenoside R1, Marmesin, Quercetin, Ginsenoside Rg1, Formononetin, Biochanin A, Nobiletin, Ginsenoside Rb1, Ginsenoside Rb1, and Neferine, were purchased from Chengdu Prifa Technology Co., Ltd (Chengdu, China). All solvents, such as ethanol, acetonitrile, formic acid, and ammonium formate, used in the study were HPLC-grade and were purchased from Thermo Fisher Scientific (Massachusetts, USA). For the chemical characterization of A&P using ultra-high-performance liquid chromatography coupled with high-resolution mass spectrometry (UPLC-HRMS), the main

components of A&P were ground into a fine powder. Then, 5 g of the A&P powder was extracted with ethanol (1:8 volume ratio) under sonication for 30 min. The mixture was centrifuged at 12,000 rpm for 15 min to obtain the ethanolic extract or supernatant A. The filter residue was then sonicated with water (1:10 volume ratio) and centrifuged at 12,000 rpm for 15 min to obtain the water extract or supernatant B. The supernatants A and B were combined in a 1:1 volume ratio and centrifuged at 12,000 rpm for 15 min. The resulting supernatant was collected as the A&P extract for subsequent UPLC-HRMS analysis. NOB standard solution preparation: Weigh 1 mg of NOB standard, dissolve with 4 mL methanol, and prepare the stock solution with the mass concentration of 250 ug/ml, take 200 ul of the standard stock solution; all the above standards were prepared as above, and centrifuged at 12000 rpm for 15 min after vortexing and shaking, and then 200 ul of the supernatant solution was transferred to the sample tube for injection, and used for the subsequent analysis by UPLC-HRMS.

UPLC-HR-MS

The chemical characterization analysis of the A&P extract was operated on Ultimate 3000 hyperbaric LC system coupled with high resolution Q-Exactive mass spectrometer *via* an electrospray ionization (ESI) interface (Thermo Fisher Scientific, Bremen, Germany), according to the methods in our previous report [28]. Following are the optimized chromatographic parameters of this study: mobile phase was composed of water (0.1% formic acid, A) mixed in gradient mode with acetonitrile (0.1% formic acid, B), at a flow rate of 200 µL/min. The elution gradient was optimized as follows: 0-5 min, 2% B; 5-8 min, 2% to 20% B; 8-45 min, 20% to 55% B; 45-52 min, 55% to 100% B; 52-58 min, 100% B. The injection volume was 2.0 µL and the sampler was set at 4 °C. Positive full scan modes within the range of m/z (mass/charge ratio) 150-1500 at a resolution of 70,000 were used for acquisition of accurate molecular ion. The other parameters were set as follows: spray voltage, +3.5 kV; sheath gas flow rate, 35 arb; aux gas flow rate, 10 arb; capillary temperature, 320 °C; vaporizer temperature, 250 °C; RF lens, 50%. Xcalibur 3.0 software (Thermo Fisher) was used for UPLC-HRMS control and data handling.

CKD-induced animal model and nobiletin (NOB) treatment

NOB was obtained from Chengdu Prifa Technology Co., Ltd (HPLC > 95% purity). Male C57BL/6 mice (8 weeks old, weighing 22-25 g) used in this study were purchased from GemPharmatech Co., Ltd. (Chengdu, China). The mice were kept under a 12-h light/12-h dark cycle and provided with unrestricted access to food and water. They were randomly divided into four groups ($n = 6$ per group): Control, CKD, CKD with low-dose treatment (50 mg/kg/day), and CKD with high-dose treatment (100 mg/kg/day). The mice were anesthetized with 1% pentobarbital sodium. The CKD mouse model was induced by ligation of the upper and lower poles of the left kidney, following the removal of the right kidney after one week, as previously described [29]. After one month, the NOB-treated groups received the respective doses by gastric gavage for a duration of four weeks. The control and CKD mice were administered with an equal volume of saline. At the end of the experimental period, all the mice were sacrificed. For histological analysis, a portion of the kidneys was fixed in 4% paraformaldehyde and embedded in paraffin according to standard procedures. The medullary part of the kidneys was removed for protein and RNA isolation, which was performed on the remaining cortex. All animal procedures were carried out in accordance with the guidelines approved by the Animal Ethics Committee of Southwest Medical University (Approval number: 20220308001).

Cell culture and transfections

The TCMK1 cells (ATCC Cat# CCL-139, United States) were obtained and cultured in DMEM (BasalMedia, Cat# L110KJ, China) supplemented with 10% Fetal Bovine Serum (FBS, Gibco, Cat# 16000-044, United States) and 1% penicillin-streptomycin (Beyotime, Cat# C0222, China). The cells were maintained at 37 °C in a 5% CO2 environment. To create a fibrotic cell model, TCMK1 cells at 80% confluence were subjected to serum starvation in a medium containing 0.5% FBS for 12 h. Subsequently, TGF-β1 was added at a concentration of 5 ng/ml to stimulate the cells for the specified duration. For plasmid transfection, TCMK1 cells at approximately 50% confluence were transfected with the Lgals-1 overexpression plasmid (pcDNA 3.1-Lgals1, 4 µg in each well) provided by Genechem (Shanghai, China) using polyethylenimine reagent. After transfection, the medium was replaced within 24 h. The cellular morphology and growth status were observed using a light microscope.

CCK-8 analysis

Cells were seeded in 96-well plates at a density of 3000 cells per well, with 3 replicate wells per group. Following 24 h of starvation culture, the cells were treated with varying concentrations of NOB for 24 h. Subsequently, the medium was removed, and 100 µl of 10% CCK-8 reagent was added to each well. The plates were then incubated in an incubator for 3 h. The absorbance of each well was measured at 450 nm using a BioTeK reader, and the cell survival rate was calculated based on these measurements.

Detection of renal function

The serum of the mice was collected to detect the creatinine (C011-1-1, Nanjing Jiancheng Bioengineering Institute) and urea nitrogen (C013-2-1, Nanjing Jiancheng Bioengineering Institute) following the instructions of corresponding kits.

Real-Time PCR

ChamQ Universal SYBR qPCR Master Mix (Q711, Vazyme) is used to detect the mRNA expression levels of cells and kidneys; TRIzol Reagent (11596026, Invitrogen, USA) was used to extract total RNA from TCMK1 cells and kidneys; HiScript® III RT SuperMix (R323, Vazyme) was used to reverse transcribe total RNA to cDNA; RT-PCR was performed with the Mastercycler ep Realplex2 real-time PCR system (LightCycle480II, Roche, USA). The relative expression of a given gene is calculated by the threshold cycle (CT) method. Primer sequences are listed in Table 1.

Histology and immunofluorescence staining

The renal tissue was embedded in paraffin using the method described previously [30]. Briefly, mouse kidney samples were isolated, embedded in paraffin, and sectioned at 4 μm for further analysis. Sections were placed in xylene for dewaxing and rehydrated in gradient ethanol, and stained in H&E and Masson's trichrome solution according to the manufacturer's instructions (Beyotime, China). Pictures were captured by the optical microscope (ICC50W, Leica). For the immunofluorescence, the kidney samples were fixed in 4% paraformaldehyde at 4 °C overnight. Then, the sections were gradient dehydrated (10-20-30% sucrose in phosphate-buffered saline (PBS)) and embedded in OCT. Subsequently, the sections were blocked with 5% BSA for 30 min, incubated with antibody against Lgals 1 (Santa Cruz, USA) followed by incubation with corresponding AlexaFluor647 conjugated secondary antibodies. Finally, the sections were photographed with a confocal microscopy (Nikon, Japan).

Western blotting

The total protein was extracted from cells and tissues using RIPA lysis buffer containing protease and phosphatase inhibitors, then quantitated by the BCA method. Proteins (70 μg of each sample) were separated on a 10% SDS-PAGE gel and transferred to a PVDF membrane by wet blotting. After blocking with 5% milk, the membranes were incubated with the antibodies against Fibronectin (Rabbit anti-mouse, T59537M, 1:1000, Abmart), Collagen I (Rabbit anti-mouse, TA7001M, 1:1000, Abmart), α-SMA (Mouse anti-mouse, BM0002, 1:1000, BOSTER), Lgals 1(Rabbit anti-mouse, 12936S, 1:1000, Cell Signaling) at 4◦C overnight. The next day, membranes were subsequently incubated with the secondary antibody of peroxidase-conjugated goat anti-mouse IgG (M214008M, 1:4000) and goat anti-rabbit IgG (M214011M, 1:4000) for 1 h at room temperature. The band was analyzed by the gel imaging system. Gray intensity of the band was calculated by ImageJ software.

Table 1. Sequence of primers for Real-time PCR.

Gene	Sequence
α-SMA	F:GTCCCAGACATCAGGGAGTAA
	R:TCGGATACTTCAGCGTCAGGA
Collagen I	F:GCTCCTCTTAGGGGCCACT
	R:CCACGTCTCACCATTGGGG
Fibronectin	F:ATGTGGACCCCTCCTGATAGT
	R:GCCCAGTGATTTCGGCAAAGG
Lgals 1	F:AACCTGGGGAATGTCTCAAAGT
	R:GGTGATGCACACCTCTGTGA
GAPDH	F:ACAGCAACAGGGTGGTGGAC
	R:TTTGAGGGTGCAGCGAACTT

Statistical analysis

This study used SPSS22.0 and Prism 6 software for analysis. Data were presented as mean ± standard error. One-way analysis of variance (One-Way ANOVA) was used for multigroup comparison. $p < 0.05$ was considered statistically significant.

Results

NOB is one of the main active ingredients of a&P

We conducted in-depth analysis of the main components of A&P using UPLC-HR-MS. The total ion chromatogram of A&P (Figure 1) was obtained. By combining the retention time of the compounds, utilizing isotopic abundance to determine the relative content of each isotope of the same element in the target monomer, comparing excimer ion peaks, collecting secondary fragments, and referring to existing literature, we analyzed a total of 13 major chemical components, including flavonoids, isoflavones, bean isoflavones, saponins, coumarins, triterpenes, sterols, and other compounds (Table 2). Furthermore, nine of these compounds were subjected to chromatographic analysis using standard reference samples. It was observed that NOB exhibited a significant peak area and a high relative percentage in the positive ion mode within the total ion chromatogram (Figure 2). Combined with the theory of traditional Chinese medicine, the main potency in the compound drug, which is usually the one that is relatively more abundant in the compound ingredient, we speculated that NOB may play a major role in improving renal fibrosis in 13 main compounds. At the same time, previous studies have reported that tangerine can reduce drug nephrotoxicity[19], so its effect of enhancing and improving renal fibrosis while reducing drug toxicity is consistent with the concept of increasing efficiency and reducing toxicity of traditional Chinese medicine, and undoubtedly becomes the focus of our research.

NOB improves renal function and pathological injury in 5/6 nephrectomy mice

The molecular structure of NOB is depicted in Figure 3A. To investigate the effects of NOB in a 5/6 nephrectomy chronic kidney disease (CKD) model, mice were administered NOB at doses of 50 and 100 mg/kg. Our data revealed that levels of creatinine (CREA) and blood urea nitrogen (BUN) were elevated in the CKD group compared to the control (Ctrl) group. However, treatment with NOB in the CKD + NOB groups

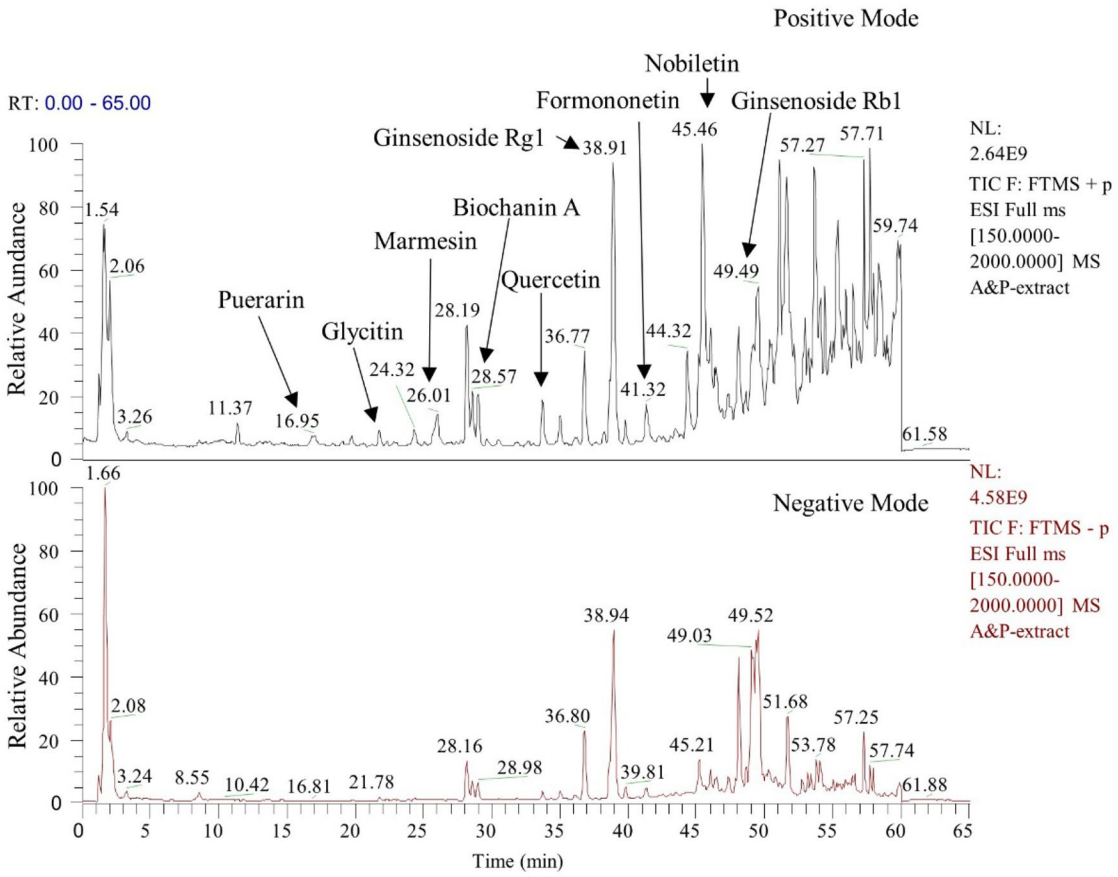

Figure 1. Typical total ion chromatograms (TIC) of a&P in the negative ion mode and positive ion mode using UPLC-HR-MS.

significantly reduced these indices, indicating that NOB effectively improved renal function in 5/6 nephrectomized mice (Figure 3B). Histological analysis using H&E staining demonstrated dilated renal tubules and glomerular sclerosis in the kidneys of mice in the CKD model group. Importantly, these pathological damages were significantly ameliorated in the NOB-treated mice. Furthermore, Masson staining, utilized to assess renal tissue fibrosis, displayed extensive interstitial fibrosis (indicated by blue-colored collagen) in the kidneys of mice in the CKD model group. However, in NOB-treated mice, collagen deposition was significantly reduced, indicating a successful attenuation of renal fibrosis in the 5/6 nephrectomy model (Figure 3C).

NOB treatment reduced 5/6 nephrectomy-induced renal fibrosis

Renal fibrosis is a significant characteristic of both the biological and pathological changes observed in patients with chronic kidney disease (CKD) [31].

In this present study, we observed a substantial upregulation in the mRNA levels of α-SMA, collagen I, and fibronectin in CKD mice. However, following treatment with NOB, the expression of these cytokines was markedly reduced (Figure 4A). These findings were further confirmed by Western blot analysis (Figure 4B, C), suggesting a positive effect of NOB on anti-fibrosis in kidney of CKD model.

NOB down-regulated Lgals1 and inhibits PI3K/AKT pathway in CKD

In our previous study, we identified Lgals1 as a crucial gene involved in the development of renal fibrosis during the transition from AKI to CKD [27]. To investigate the role of Lgals1 as a key gene in renal fibrosis, we assessed its expression *in vivo* using immunohistochemical staining. The results revealed a significant upregulation of Lgals1 in interstitial deposits of CKD mice induced by 5/6 nephrectomy. However, after treatment with NOB, the expression of Lgals1 was markedly reduced (Figure 5A). Considering that the PI3K/AKT signaling pathway is known to regulate renal fibrosis processes, we examined the impact of NOB treatment on this pathway using Western blot analysis. We observed that treatment with NOB in CKD mice led to dose-dependent decreases in the levels of phosphorylated PI3K (p-PI3K), phosphorylated AKT (p-AKT), and Gal-1, indicating the modulation of this pathway by NOB in reducing renal fibrosis (Figure 5B-E).

Table 2. UPLC-HR-MS data of 13 compounds in A&P.

NO.	T_R(min)	Ion form	Measured mass	Formula	Error(ppm)	MS/MS fragments	Identification	Type
1	13.6	$[M+H]^+$	307.07922	$C_{15}H_{14}O_7$	−1.42	248.09178 202.08620 150.05498 105.03382 71.04975	(-)-Epigallocatechin	Flavonoids
2	16.57	$[M+H]^+$	417.11792	$C_{21}H_{20}O_9$	−1.12	399.10739 381.09671 297.07559 268.07285 267.06566	Puerarin	Isoflavones
3	21.81	$[M+H]^+$	447.12860	$C_{22}H_{22}O_{10}$	2.540	285.07523 270.05194 253.04918 225.05437 137.02318	Glycitin	Soy Isoflavones
4	36.73	$[M+H]^+$	933.54047	$C_{37}H_{62}O_{10}$	−2.651	931.52521 637.43030 113.02256 89.02263 71.01214	Notoginsenoside R1	Saponins
5	26.02	$[M+H]^+$	247.09396	$C_{14}H_{14}O_4$	−1.75	299.08476 214.06136 176.04588 175.03813 55.01819	Mamesin	Coumarins
6	22.35	$[M+H]^+$	303.04965	$C_{15}H_{10}O_7$	−1.98	257.04437 229.04974 201.05489 153.01834 137.02374	Quercetin	Flavonoids
7	38.96	$[M+Na]^+$	823.47711	$C_{42}H_{72}O_{14}$	−1.02	750.33563 643.41766 463.35315 221.06216 203.05255	Ginsenoside Rg1	Triterpenoids
8	41.32	$[M+H]^+$	269.08035	$C_{16}H_{12}O_4$	−2.00	254.05710 237.05443 226.06223 213.09082 118.04142	Fomononetin	Isoflavones
9	28.5	$[M+H]^+$	285.07520	$C_{16}H_{12}O_5$	−1.99	270.05203 253.04929 225.05450 213.05450 137.02328	Biochanin A	Isoflavones
10	46.05	$[M+H]^+$	403.13821	$C_{21}H_{22}O_8$	−1.90	388.11499 373.09158 327.08606 211.02359 183.02875	Nobiletin	Flavonoids
11	49.39	$[M+Na]^+$	1131.58765	$C_{54}H_{92}O_{63}$	−.309	789.47455 365.10513 305.08386 245.06406 203.05196	Ginsenoside Rb1	Steroid
12	52.25	$[M+H]^+$	391.24542	$C_{23}H_{34}O_5$	−2.60	216.98979 167.03326 155.27763 149.02321 95.04952	Tussilagone	Sesquiterpene
13	54.35	$[M+H]^+$	625.32300	$C_{38}H_{44}N_2O_6$	1.36	593.28986 463.26639 445.25613 403.18777 203.05266	Neferine	Alkaloids

NOB inhibited the TGF-β induced fibrosis in TCMK-1 cells

To assess the impact on cell viability, TCMK-1 cells were exposed to various concentrations of NOB. The cytotoxicity of NOB was determined using a CCK-8 assay, and the results demonstrated no significant cytotoxic effects at concentrations below 100 μM (Figure 6A). Subsequently, we investigated the anti-fibrotic effects of NOB *in vitro*. Real-time PCR

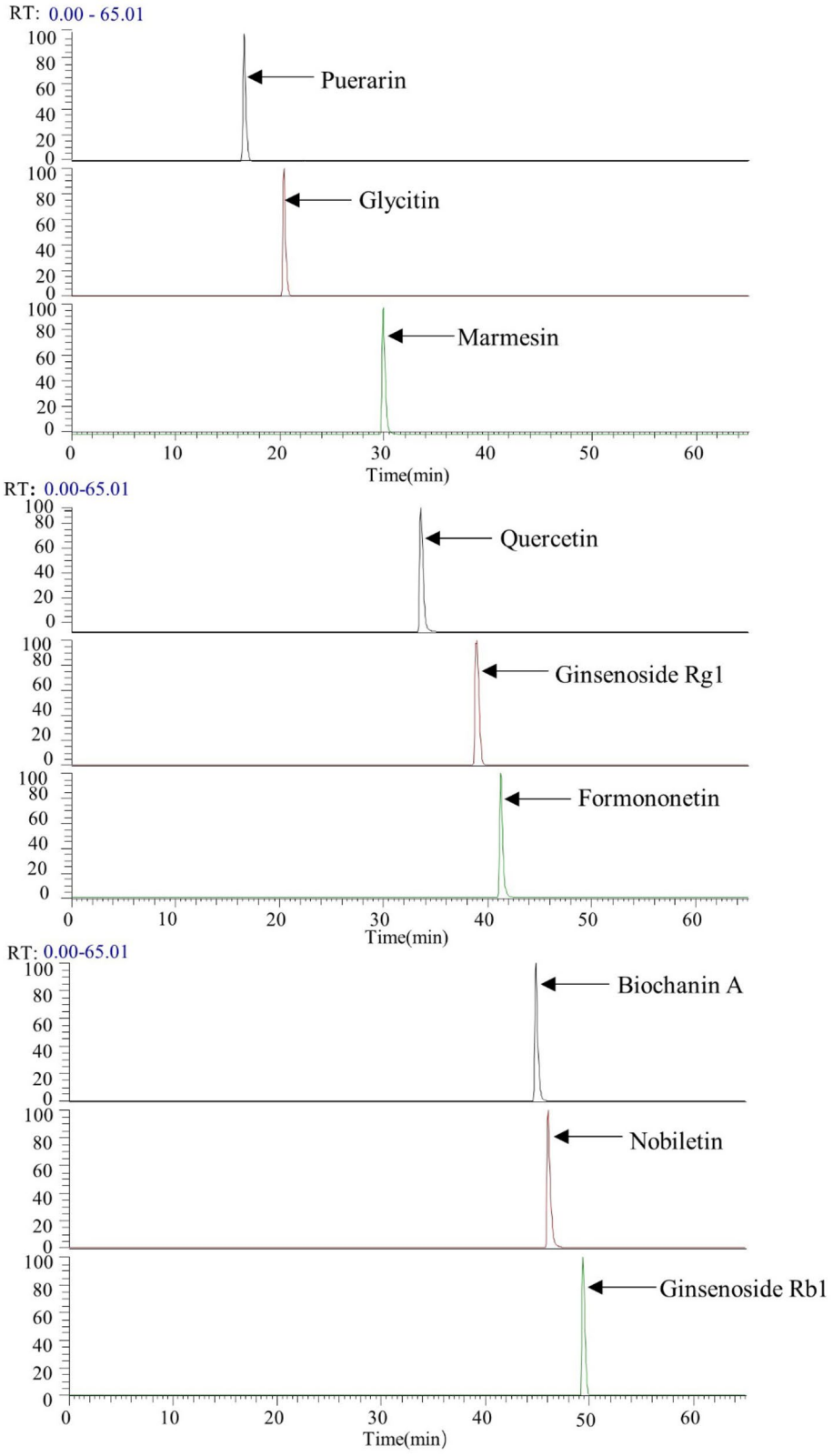

Figure 2. Extracted ion chromatograms of the 9 standard substances in the positive ion mode of UPLC-HR-MS.

analysis revealed that NOB treatment significantly reduced the mRNA expression of fibrotic markers, including Fibronectin and Collagen I, in TGF-β-induced TCMK-1 cells (Figure 6B). Correspondingly, Western blot analysis confirmed a consistent reduction in the protein levels of these markers (Figure 6C, D).

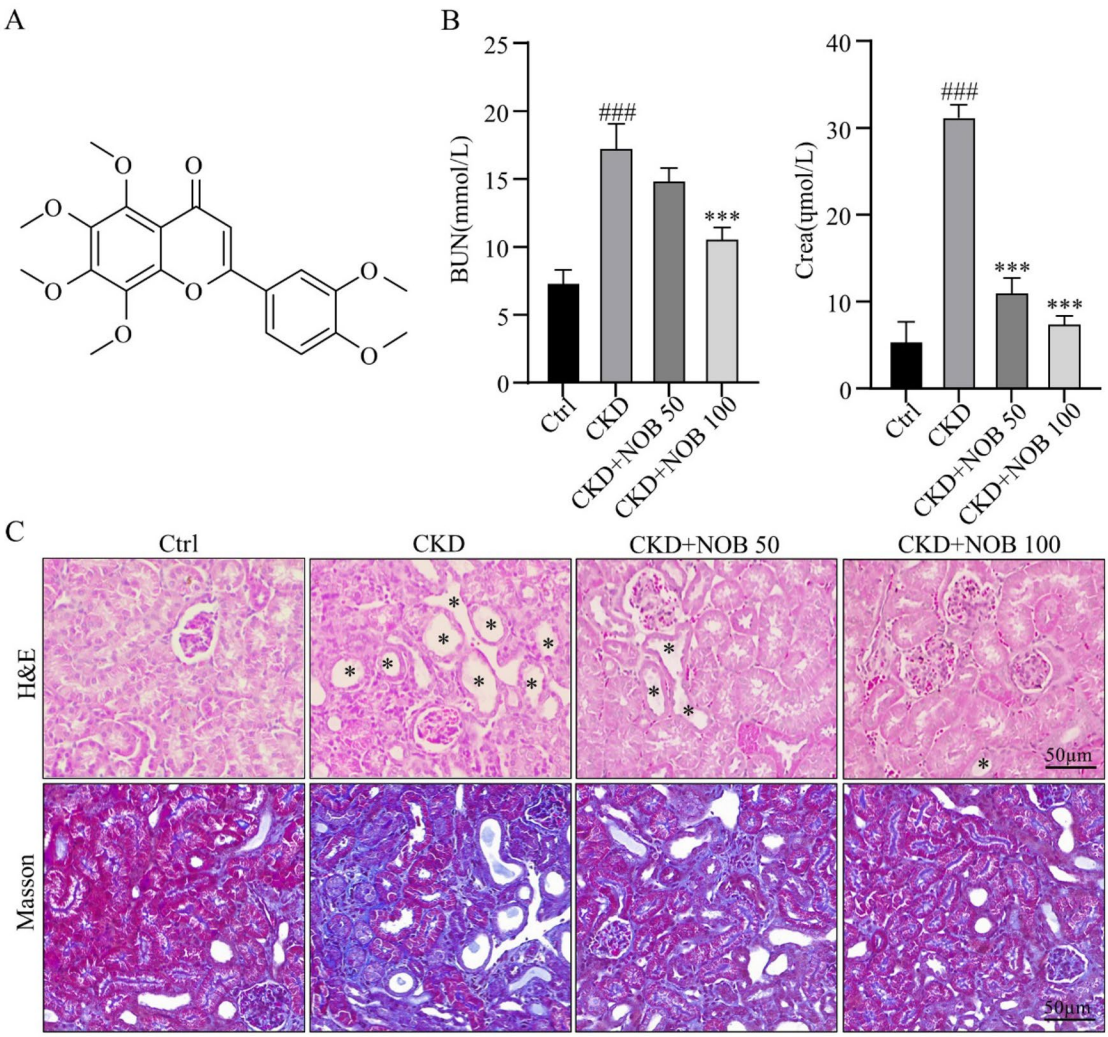

Figure 3. NOB improves renal function and pathological injury in 5/6 nephrectomy mice. (A) The chemical molecular structure of NOB; (B) The results of serum urea nitrogen and creatinine in each group; (C) The pathological staining of kidney in all groups of mice (H&E staining and Masson staining, the asterisk marks the damaged renal tubules). $^{###}p < 0.001$ vs ctrl, $^{***}p < 0.001$ vs CKD.

NOB inhibited the mRNA and protein levels of Lgals1, PI3K and AKT signaling in TGF-β-induced TCMK-1

The PI3K/AKT signaling pathway plays a crucial role in regulating renal fibrosis, and we previously established the association of Lgals1 with CKD *in vivo*. To further investigate our hypothesis, we examined the effects of NOB on Lgals1 and the PI3K/AKT pathway in TCMK-1 cells. Real-time PCR was conducted to assess the expression of Lgals1 mRNA, while Western blot analysis were performed to measure the protein levels of phosphorylated PI3K, AKT, and Gal-1. Stimulation of TCMK-1 cells with TGF-β led to a substantial increase in the expression of Lgals1 mRNA, Gal-1 protein, as well as the phosphorylation of PI3K and AKT. However, treatment with NOB effectively suppressed the TGF-β-induced upregulation of Lgals1 mRNA, Gal-1 protein, p-PI3K, and p-AKT in TCMK-1 cells (Figure 7A-C).

NOB suppressed the fibrosis and activation of PI3K/AKT signaling induced by overexpression of Lgals1

To further investigate whether Lgals1 is a key gene involved in renal fibrosis during CKD, we overexpressed Lgals 1 in TCMK-1 cells by transfecting the pcDNA 3.1-Lgals1plasmid. The levels of α-SMA, collagen I and fibronectin were significantly increased in the plasmid transfected group (Lgals1-OE) compared to Ctrl group, and the trend of the above fibrotic protein expression was strongly blocked when treated with 80μM NOB tested by Western blot (Figure 8 A, B), suggesting that Lgals1 may be a key gene regulating renal fibrosis in CKD. In addition, to verify the involvement of Lgals1 in regulating the activation of PI3K/AKT signaling pathway, we performed the Western blot on each group. The results showed that the expression of Gal-1, p-PI3K, and p-AKT was significantly increased in the plasmid-transfected group (Lgals1-OE) in TCMK-1 compared with Ctrl group, while when further treated with 80μM NOB significantly down-

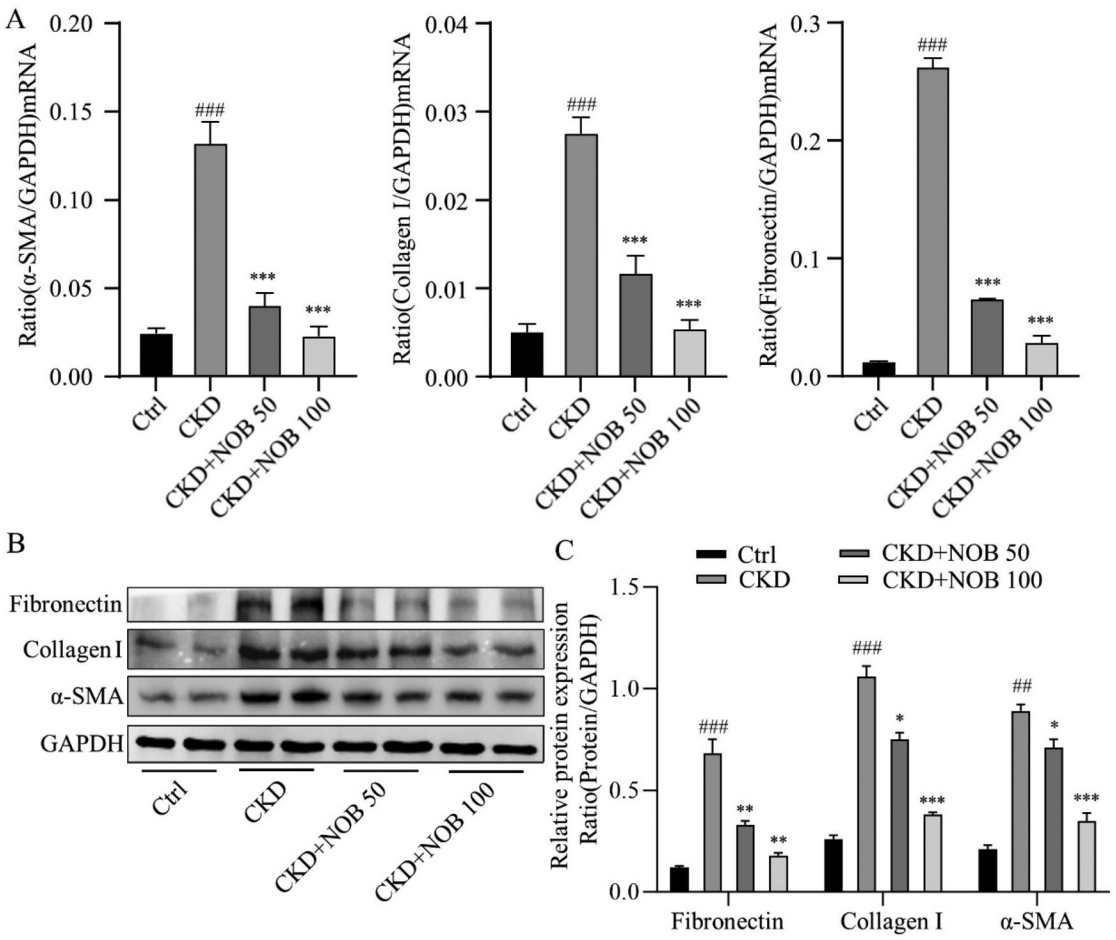

Figure 4. NOB treatment reduced 5/6 nephrectomy-induced renal fibrosis. (A) The mRNA expression of fibrosis indicators tested by real-time PCR; (B, C) the protein levels of fibrosis indicators in the kidney of each group of mice. $^{\#\#}p < 0.01$, $^{\#\#\#}p < 0.001$ vs ctrl; $^{*}p < 0.05$, $^{**}p < 0.01$, $^{***}p < 0.001$ vs CKD.

regulated p-PI3K, p-AKT expression levels (Figure 8 C, D). These results suggest that in TCMK-1, Lgals1 induces the formation of renal fibrosis in CKD through activation of the PI3K/AKT signaling pathway, and that treatment with NOB ameliorates this lesion process.

Discussion

Renal fibrosis, a prominent feature of CKD, has emerged as a potential therapeutic target [32]. Exploring natural compounds as therapeutic options for renal fibrosis in CKD has gained significant attention in global research [33]. In our previous clinical practice and preliminary experiments, we obtained a substantial amount of data that confirmed the effectiveness of A&P in alleviating CKD fibrosis and preserving residual kidney function [7, 34]. A&P is primarily composed of *Astragalus mongholicus Bunge*, *Panax notoginseng*, *Angelica sinensis*, *Achyranthes bidentata Blume*, and *Ecklonia kurome Okamura* [7]. To better understand the complex chemical composition of A&P, in this study, multiple components of A&P could be separated simultaneously and efficiently by UPLC-HR-MS, and 13 major components were identified from its extracts, and then by analyzing the ionic fragments of the components of the A&P compound in comparison with the 13 standards, it provided a reference for the identification of the components of A&P as well as the improvement of its quality control standards. Meawhile, we discovered that NOB is a key flavonoid compound with significant therapeutic potential. Notably, NOB not only exhibits anti-kidney fibrosis effects but also mitigates the toxicity of other drugs, aligning with the principles of traditional Chinese medicine wherein it possesses both efficacy and detoxification properties [18, 19, 35, 36]. Progressive CKD, characterized by interstitial fibrosis, can lead to tubular atrophy, renal functional loss, and end-stage renal failure [37]. Our experimental findings demonstrate that NOB effectively delays the progression of renal dysfunction and reduces renal pathological damage *in vivo*. Furthermore, NOB ameliorates interstitial fibrosis both *in vitro* and *in vivo* by inhibiting the activation of the PI3K/AKT pathway, thereby downregulating the expression of fibrogenic factors through its targeting of LGALS1.

As a flavonoid compound, NOB possesses a range of pharmacological properties, including anti-inflammatory, antioxidant, and anti-tumor characteristics [38, 39]. Additionally, evidence suggests that NOB has significant renal protective effects against drug-induced nephrotoxicity and inflammation-related reactions [17, 35, 40–42]. Notably, NOB exhibits additional beneficial bioactivities, such as vascular endothelial protection, modulation of

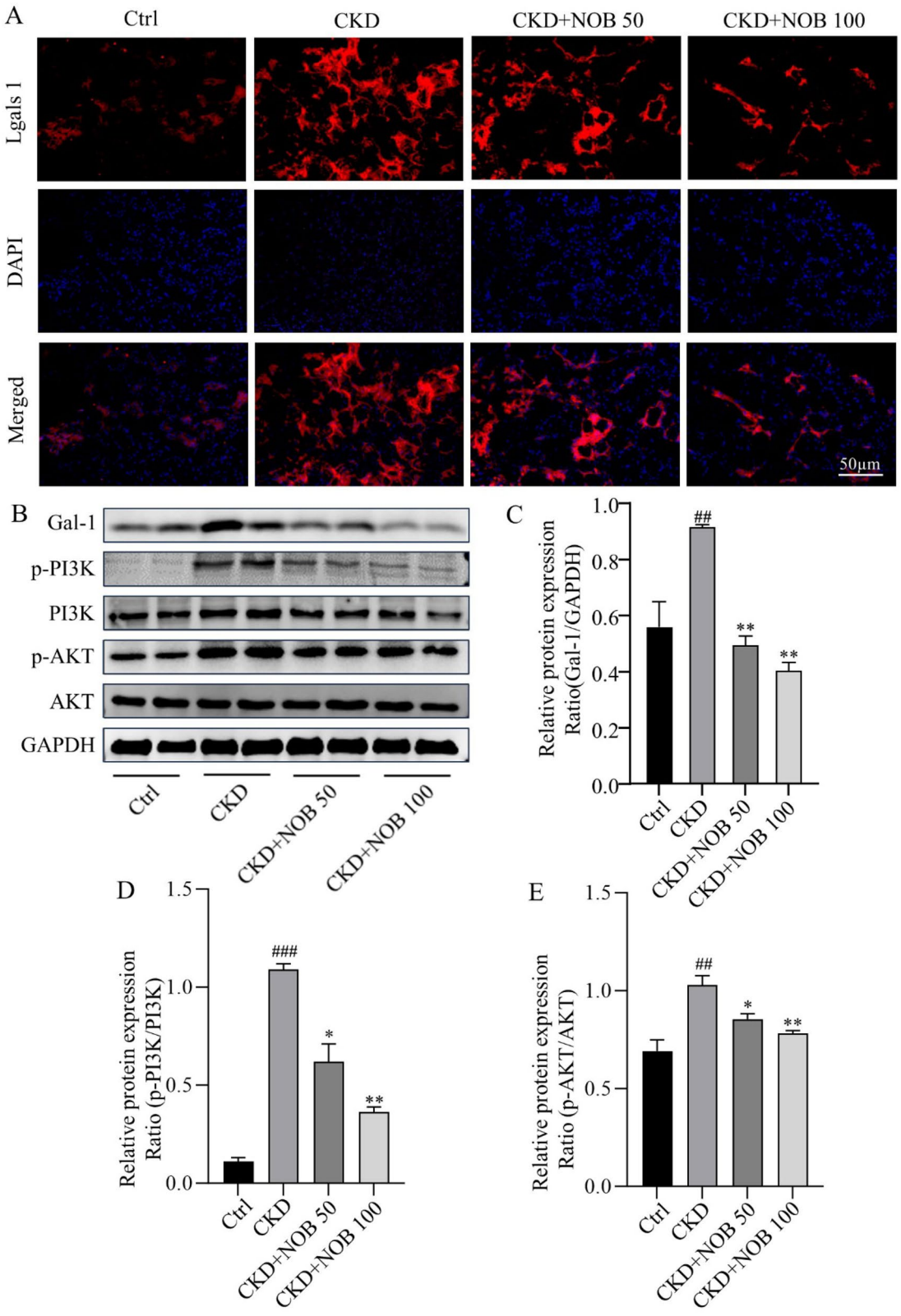

Figure 5. NOB down-regulated Lgals1 and inhibits PI3K/AKT pathway in CKD. (A) The immunofluorescent staining of Lgals 1 in the kidney tissue of each group of mice; (B-E) the protein levels of Gal-1, p-PI3K, PI3K, p-AKT and AKT in the kidney cortex of each group of mice by Western blot. $^{\#\#}p < 0.01$, $^{\#\#\#}p < 0.001$ vs ctrl; $^{*}p < 0.05$, $^{**}p < 0.01$ vs CKD.

gut microbiota homeostasis, and anti-multi-organ fibrosis properties, which position it as a promising candidate in the search for effective treatments against renal fibrosis [43–45]. To gain a deeper understanding of the effects of NOB, our laboratory conducted comprehensive examinations of biochemical markers and pathological changes in mice with 5/6 nephrectomy. The results

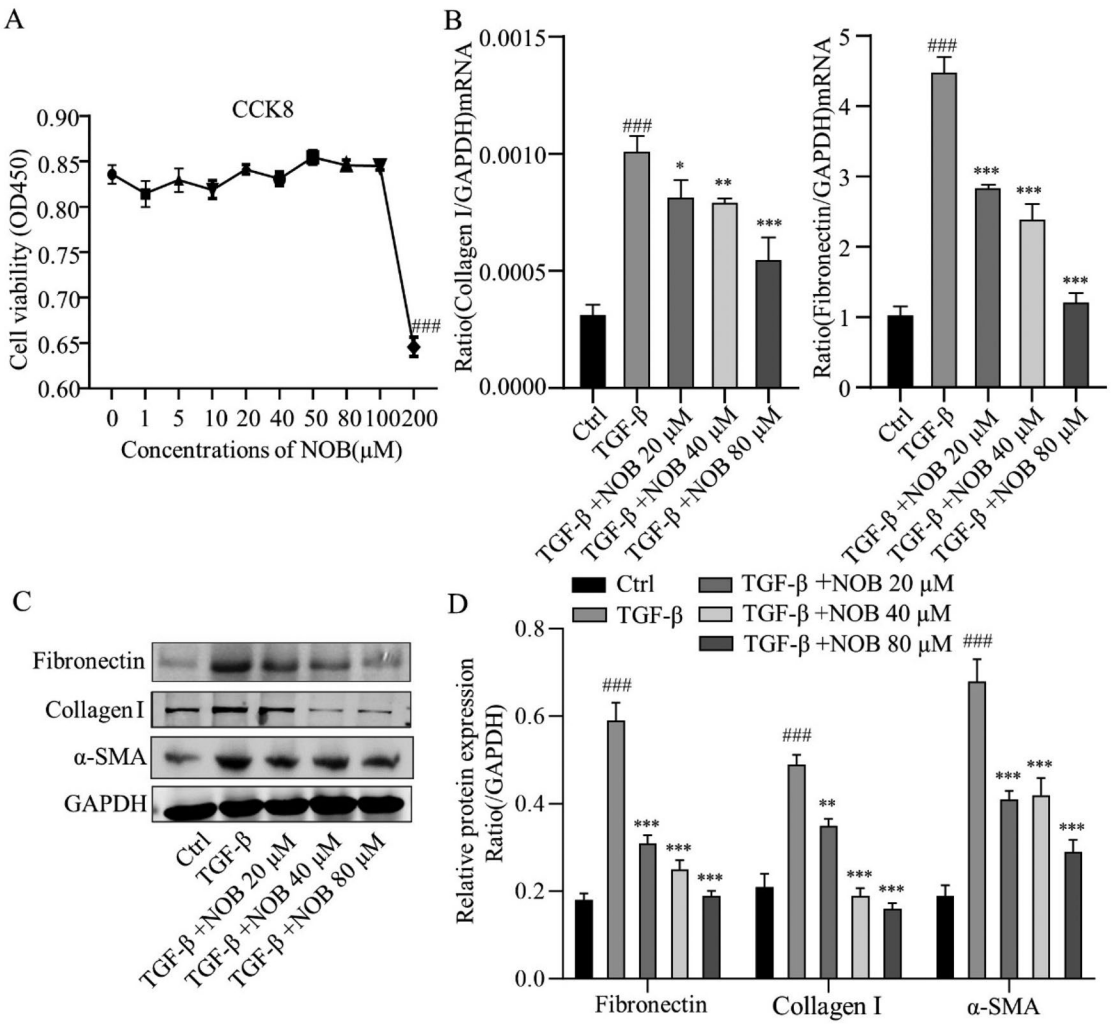

Figure 6. NOB inhibited the TGF-β induced fibrosis in TCMK-1 cells. (A) The statistical results of the effect of different concentrations of NOB on the viability of TCMK-1 cells ($^{###}p < 0.001$ vs blank); (B) The mRNA expression of fibrosis indicators in TCMK-1 cells detected by real-time PCR; (C, D) The protein levels of fibrosis indicators in TCMK-1 cells by Western blot. $^{###}p < 0.001$ vs ctrl; $^{*}p < 0.05$, $^{**}p < 0.01$, $^{***}p < 0.001$ vs TGF-β.

confirmed that NOB treatment led to a dose-dependent reduction in CREA and BUN levels compared to the CKD group. Additionally, H&E and Masson's staining revealed improved renal pathological structure in the kidneys of NOB-treated mice, with noticeable reductions in interstitial fibrosis factor expression.

Persistent inflammation is a key contributing factor to renal fibrosis, as uncontrolled inflammation infiltrates the kidney, leading to excessive production and deposition of extracellular matrix (ECM) and tissue fibrosis accumulation. Resident fibroblasts play a central role in this process, undergoing differentiation into active myofibroblasts and expressing α-SMA, Collagen I, and Fibronectin [46, 47]. The pro-fibrotic cytokine TGF-β is primarily responsible for inducing myofibroblast differentiation and promoting Collagen I deposition [47]. Through our experiments, we observed a substantial increase in α-SMA, Collagen I, and Fibronectin expression in the CKD group both *in vivo* and *in vitro*. However, following NOB treatment, we observed a dose-dependent reduction in the expression levels of these markers, as confirmed by Real-time PCR and Western blot analysis. These findings suggest that NOB exhibits a renoprotective effect by attenuating the expression of α-SMA, Collagen I, and Fibronectin.

Gal-1, encoded by Lgals1, is the founding member of the galectin family, functioning as a lectin with a highly conserved carbohydrate recognition domain and an affinity for β-galactose-containing oligosaccharides [48]. Recent studies have revealed the involvement of Gal-1 as a novel fibrotic protein in the regulation of anti-inflammation, tissue repair, and epithelial regeneration [21, 22]. In our previous research utilizing weighted gene co-expression network analysis (WGCNA), we identified Lgals1 as a key gene in renal fibrosis following acute kidney injury [27]. Additionally, Gal-1 has been found to be upregulated in the kidneys of diabetic mice and renal tubular cells exposed to high glucose, indicating its potential role in renal fibrosis in the context of diabetes [21]. In this present study, we found a high level of

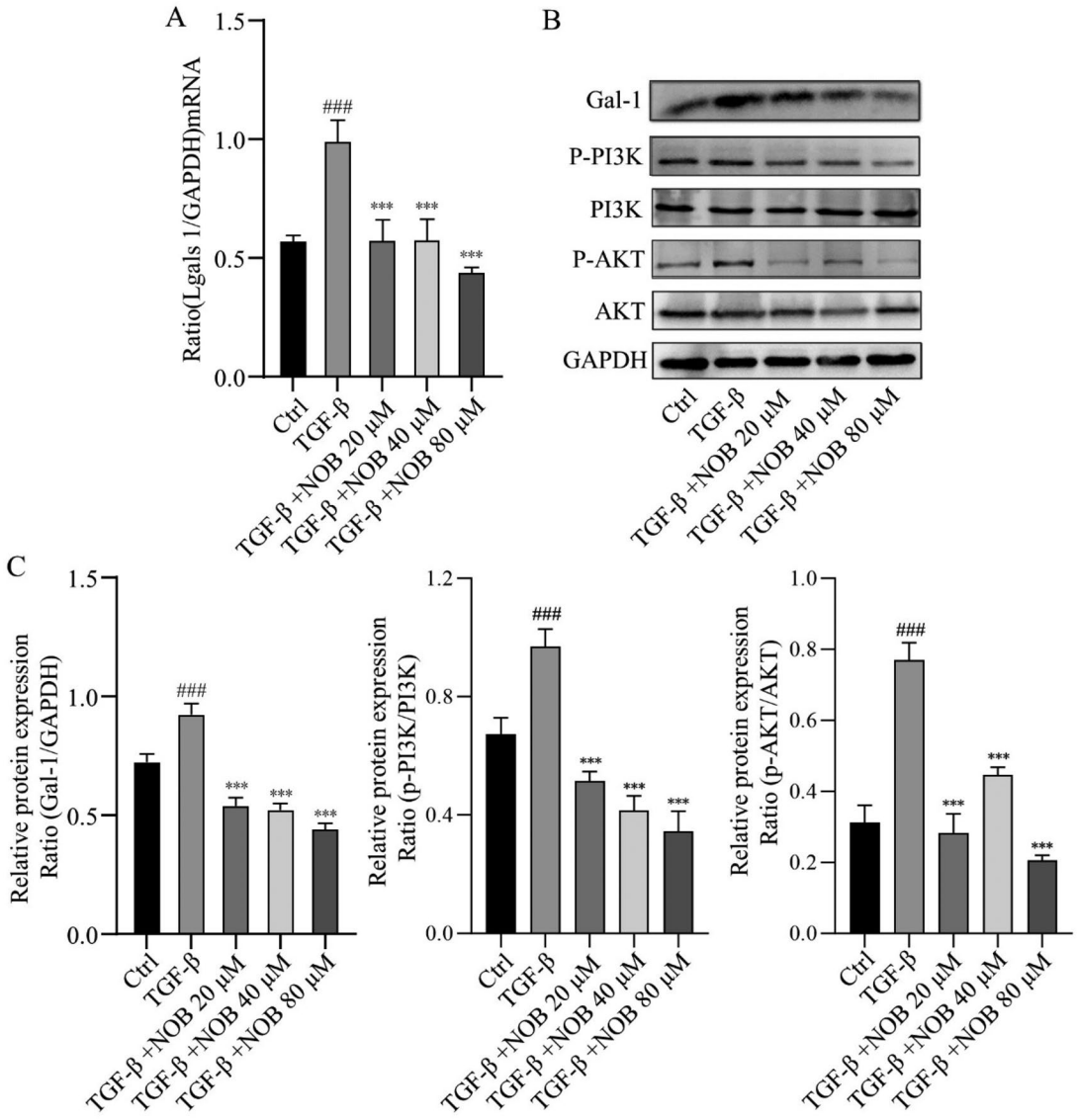

Figure 7. NOB inhibited the mRNA and protein levels of Lgals1, PI3K and AKT signaling in TGF-β-induced TCMK-1. (A) The mRNA expression of Lgals1 in TCMK-1 cells. (B, C) The Western blot assay of Gal-1 and PI3K/AKT pathway protein expression in TCMK-1 cells. $^{###}p < 0.001$ vs ctrl; $^{***}p < 0.001$ vs TGF-β.

Gal-1 protein in kidney of CKD mice and TGF-β-induced TCMK1 cells. Furthermore, overexpression of Lgals1 through plasmid transfection resulted in a significant upregulation of α-SMA, Collagen I, and Fibronectin in cells. These findings provide evidences that Gal-1 is involved in the regulation of renal fibrosis in CKD. Notably, treatment with NOB led to a significant downregulation of Gal-1 expression at both the protein and gene levels, as observed through immunofluorescence, Real-time PCR, and Western blotting. This suggests that NOB may target the Lgals1 gene, thereby suppressing Gal-1 protein expression. Consequently, Gal-1 may serve as a potential biomarker for renal fibrosis and represents an appealing target for anti-fibrotic interventions, holding promise for future applications in the treatment of fibrotic diseases.

A recent study demonstrated that the overexpression of Gal-1 activates the FAK/PI3K/AKT pathway by upregulating αvβ3 integrin expression, thereby promoting hepatocellular carcinoma invasion *via* the epithelial-mesenchymal transition (EMT) process [25]. Additionally, Gal-1 has been shown to inhibit PDGF-BB-induced proliferation and migration of airway smooth muscle cells by suppressing the PI3K/AKT signaling pathway [49]. Furthermore, the reciprocal feedback between overexpression of Lgals1 and the AKT signaling pathway may contribute to scar tissue formation [21]. In our study, we observed elevated expression levels of Gal-1, p-PI3K, and p-AKT in the kidneys of the CKD model through Real-time PCR and Western blotting analysis. However, following NOB treatment, these expression levels were significantly reduced. *In vitro* experiments conducted on TCMK-1 cells showed that overexpression of Lgals1 led to the activation of PI3K and AKT phosphorylation, but treatment with NOB strongly downregulated the expression levels of p-PI3K and p-AKT *in vivo* and *in vitro*. These findings suggest that NOB protects kidney in CKD through inhibiting of Gal-1 regulated PI3K and AKT.

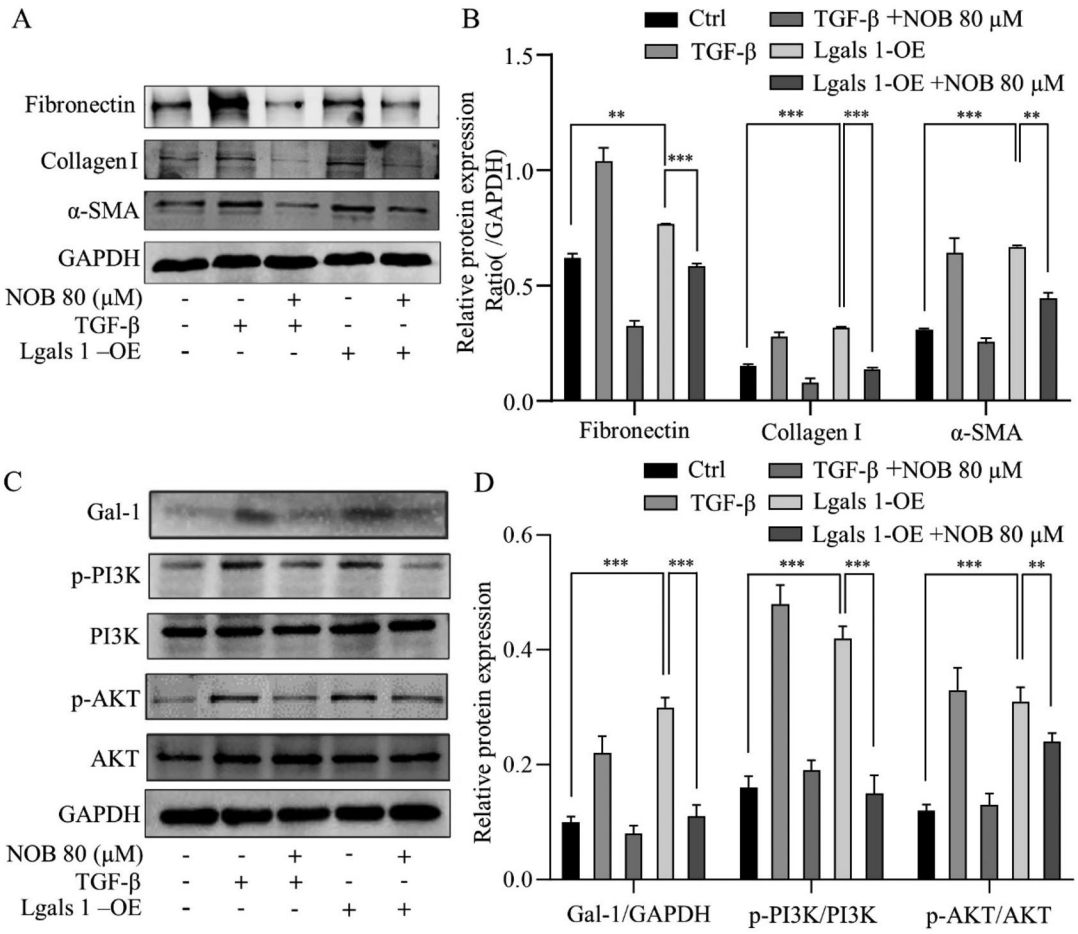

Figure 8. NOB suppressed the fibrosis and activation of PI3K/AKT signaling induced by overexpression of Lgals1. (A, B) The Western blot detection of fibrosis-related protein expression after transfection with Lgals-1 plasmid. (C, D) The Western blot detection of PI3K/AKT pathway-related protein expression after transfection with Lgals-1 plasmid. $^{**}p < 0.01$, $^{***}p < 0.001$.

Conclusions

In summary, our experimental analysis focused on several components of A&P and revealed that the primary active ingredient, NOB, possesses the ability to alleviate renal fibrosis induced by 5/6 nephrectomy in chronic kidney disease (CKD). The underlying mechanism suggests that NOB exerts its anti-fibrotic effects by inhibiting the activation of the PI3K/AKT signaling pathway through the regulation of Lgals1, a key gene associated with renal fibrosis. These findings demonstrate the potential of NOB as a therapeutic intervention for clinicians in the treatment of CKD, offering the ability to mitigate fibrosis, protect renal function, and delay disease progression.

Disclosure statement

All authors declare that there are no competing interests.

Funding

This study was supported by the Sichuan Science and Technology Program (2022YFS0621, 2022NSFSC1459), the Luzhou-Southwest Medical University Science and Technology Strategic Cooperation Project (2021LZXNYD-P04, 2021LZXNYD-J02), the Innovation Team of Affiliated Traditional Medicine Hospital of Southwest Medical University (2022-CXTD-03).

ORCID

Junming Fan http://orcid.org/0000-0003-2213-4782

References

[1] Wang L, Xu X, Zhang M, et al. Prevalence of chronic kidney disease in China: results from the sixth China chronic disease and risk factor surveillance. JAMA Intern Med. 2023; 183(4):1–16. doi: 10.1001/jamainternmed.2022.6817.

[2] Yuan Q, Tan RJ, Liu Y. Myofibroblast in kidney fibrosis: origin, activation, and regulation. Adv Exp Med Biol. 2019;1165:253–283. doi: 10.1007/978-981-13-8871-2_12.

[3] Chung VCH, Wong CHL, Zhong CCW, et al. Traditional and complementary medicine for promoting healthy ageing in WHO Western Pacific Region: policy implications from utilization patterns and current evidence. Integr Med Res. 2021;10(1):100469. doi: 10.1016/j.imr.2020.100469.

[4] Mao N, Zheng YH, Zhou Y, et al. Clinical efficacy analysis of Renal Impotence Formula in the treatment of non-dialysis patients with chronic kidney disease stage 3-5. World Chin Med. 2018;13(11):2807–2810. +2814.
[5] Xie XS, Wang BF, Wang YJ, et al. Clinical efficacy observation of *Astragalus mongholicus Bunge* and *Panax notoginseng* formula in primary nephrotic syndrome. Chin J Integr Chin Western Med Nephrol. 2012;13(15):417–419.
[6] Hui D, Rui-Zhi T, Jian-Chun L, et al. *Astragalus propinquus* Schischkin and Panax notoginseng (A&P) compound relieved cisplatin-induced acute kidney injury through inhibiting the mincle maintained macrophage inflammation. J Ethnopharmacol. 2020;252:112637. doi: 10.1016/j.jep.2020.112637.
[7] Wen D, Tan R-Z, Zhao C-Y, et al. *Astragalus mongholicus Bunge* and *Panax notoginseng* (Burkill) F.H. Chen formula for renal injury in diabetic nephropathy-in vivo and in vitro evidence for autophagy regulation. Front Pharmacol. 2020;11:732. doi: 10.3389/fphar.2020.00732.
[8] Gandhi GR, Vasconcelos ABS, Wu D-T, et al. Citrus flavonoids as promising phytochemicals targeting diabetes and related complications: a systematic review of in vitro and in vivo studies. Nutrients. 2020;12(10):2907. doi: 10.3390/nu12102907.
[9] Shen J, Shan J, Zhong L, et al. Dietary phytochemicals that can extend longevity by regulation of metabolism. Plant Foods Hum Nutr. 2022;77(1):12–19. doi: 10.1007/s11130-021-00946-z.
[10] Ali AM, Gabbar MA, Abdel-Twab SM, et al. Antidiabetic potency, antioxidant effects, and mode of actions of citrus reticulata fruit peel hydroethanolic extract, hesperidin, and quercetin in nicotinamide/streptozotocin-induced wistar diabetic rats. Oxid Med Cell Longev. 2020;2020:1730492–1730421. doi: 10.1155/2020/1730492.
[11] Kim YJ, Choi MS, Woo JT, et al. Long-term dietary supplementation with low-dose nobiletin ameliorates hepatic steatosis, insulin resistance, and inflammation without altering fat mass in diet-induced obesity. Mol Nutr Food Res. 2017;61(8):1600889. doi: 10.1002/mnfr.201600889.
[12] Kanda K, Nishi K, Kadota A, et al. Nobiletin suppresses adipocyte differentiation of 3T3-L1 cells by an insulin and IBMX mixture induction. Biochim Biophys Acta. 2012;1820(4):461–468. doi: 10.1016/j.bbagen.2011.11.015.
[13] Xiong X, Kiperman T, Li W, et al. The clock-modulatory activity of Nobiletin suppresses adipogenesis via Wnt signaling. Endocrinology. 2023;164(8):bqad096. doi: 10.1210/endocr/bqad096.
[14] Mahmoud AM, Hernández Bautista RJ, Sandhu MA, et al. Beneficial effects of citrus flavonoids on cardiovascular and metabolic health. Oxid Med Cell Longev. 2019;2019:5484138–5484119. doi: 10.1155/2019/5484138.
[15] Parkar NA, Bhatt LK, Addepalli V. Efficacy of nobiletin, a citrus flavonoid, in the treatment of the cardiovascular dysfunction of diabetes in rats. Food Funct. 2016;7(7):3121–3129. doi: 10.1039/c6fo00294c.
[16] Liu B, Deng Q, Zhang L, et al. Nobiletin alleviates ischemia/reperfusion injury in the kidney by activating PI3K/AKT pathway. Mol Med Rep. 2020;22(6):4655–4662. doi: 10.3892/mmr.2020.11554.
[17] Güvenç M, Cellat M, Uyar A, et al. Nobiletin protects from renal ischemia-reperfusion injury in rats by suppressing inflammatory cytokines and regulating iNOS-eNOS expressions. Inflammation. 2020;43(1):336–346. doi: 10.1007/s10753-019-01123-w.
[18] Lo Y-H, Yang S-F, Cheng C-C, et al. Nobiletin alleviates ferroptosis-associated renal injury, inflammation, and fibrosis in a unilateral ureteral obstruction mouse model. Biomedicines. 2022;10(3):595. doi: 10.3390/biomedicines10030595.
[19] Song Y, Liu L, Liu B, et al. Interaction of nobiletin with methotrexate ameliorates 7-OH methotrexate-induced nephrotoxicity through endoplasmic reticulum stress-dependent PERK/CHOP signaling pathway. Pharmacol Res. 2021;165:105371. doi: 10.1016/j.phrs.2020.105371.
[20] Wu D, Kanda A, Liu Y, et al. Galectin-1 promotes choroidal neovascularization and subretinal fibrosis mediated via epithelial-mesenchymal transition. Faseb J. 2019;33(2):2498–2513. doi: 10.1096/fj.201801227R.
[21] Al-Obaidi N, Mohan S, Liang S, et al. Galectin-1 is a new fibrosis protein in type 1 and type 2 diabetes. FASEB J. 2019;33(1):373–387. doi: 10.1096/fj.201800555RR.
[22] Hermenean A, Oatis D, Herman H, et al. Galectin 1-A key player between tissue repair and fibrosis. Int J Mol Sci. 2022;23(10):5548. doi: 10.3390/ijms23105548.
[23] Arciniegas E, Carrillo LM, Rojas H, et al. Galectin-1 and galectin-3 and their potential binding partners in the dermal thickening of keloid tissues. Am J Dermatopathol. 2019;41(3):193–204. doi: 10.1097/DAD.0000000000001284.
[24] White NMA, Masui O, Newsted D, et al. Galectin-1 has potential prognostic significance and is implicated in clear cell renal cell carcinoma progression through the HIF/mTOR signaling axis. Br J Cancer. 2014;110(5):1250–1259. doi: 10.1038/bjc.2013.828.
[25] Zhang P-F, Li K-S, Shen Y-H, et al. Galectin-1 induces hepatocellular carcinoma EMT and sorafenib resistance by activating FAK/PI3K/AKT signaling. Cell Death Dis. 2016;7(4):e2201–e2201. doi: 10.1038/cddis.2015.324.
[26] Zhang H, Zhou Y, Wen D, et al. Noncoding RNAs: master regulator of fibroblast to myofibroblast transition in fibrosis. Int J Mol Sci. 2023;24(2):1801. doi: 10.3390/ijms24021801.
[27] Lin X, Li J, Tan R, et al. Identification of hub genes associated with the development of acute kidney injury by weighted gene co-expression network analysis. Kidney Blood Press Res. 2021;46(1):63–73. doi: 10.1159/000511661.
[28] Mazhar M, Yang G, Mao L, et al. Zhilong Huoxue Tongyu capsules ameliorate early brain inflammatory injury induced by intracerebral hemorrhage via inhibition of canonical NFsmall ka, cyrillicbeta signalling pathway. Front Pharmacol. 2022;13:850060. doi: 10.3389/fphar.2022.850060.
[29] Tan R-Z, Zhong X, Li J-C, et al. An optimized 5/6 nephrectomy mouse model based on unilateral kidney ligation and its application in renal fibrosis research. Ren Fail. 2019;41(1):555–566. doi: 10.1080/0886022X.2019.1627220.
[30] Yang J, Li J, Tan R, et al. Protocatechualdehyde attenuates obstructive nephropathy through inhibiting lncRNA9884 induced inflammation. Phytother Res. 2021;35(3):1521–1533. doi: 10.1002/ptr.6919.
[31] Liu F, Zhuang S. New therapies for the treatment of renal fibrosis. Adv Exp Med Biol. 2019;1165:625–659. doi: 10.1007/978-981-13-8871-2_31.

[32] Klinkhammer BM, Goldschmeding R, Floege J, et al. Treatment of renal fibrosis-turning challenges into opportunities. Adv Chronic Kidney Dis. 2017;24(2):117–129. doi: 10.1053/j.ackd.2016.11.002.
[33] Nastase MV, Zeng-Brouwers J, Wygrecka M, et al. Targeting renal fibrosis: mechanisms and drug delivery systems. Adv Drug Deliv Rev. 2018;129:295–307. doi: 10.1016/j.addr.2017.12.019.
[34] Rui-Zhi T, Hui D, Jian-Chun L, et al. *Astragalus mongholicus Bunge* and *Panax notoginseng* formula (A&P) combined with bifidobacterium contribute a renoprotective effect in chronic kidney disease through inhibiting macrophage inflammatory response in kidney and intestine. Front Physiol. 2020;11:583668. doi: 10.3389/fphys.2020.583668.
[35] Bunbupha S, Apaijit K, Maneesai P, et al. Nobiletin ameliorates high-fat diet-induced vascular and renal changes by reducing inflammation with modulating AdipoR1 and TGF-β1 expression in rats. Life Sci. 2020;260:118398. doi: 10.1016/j.lfs.2020.118398.
[36] Iampanichakul M, Poasakate A, Potue P, et al. Nobiletin resolves left ventricular and renal changes in 2K-1C hypertensive rats. Sci Rep. 2022;12(1):9289. doi: 10.1038/s41598-022-13513-6.
[37] Djudjaj S, Boor P. Cellular and molecular mechanisms of kidney fibrosis. Mol Aspects Med. 2019;65:16–36. doi: 10.1016/j.mam.2018.06.002.
[38] Hagenlocher Y, Gommeringer S, Held A, et al. Nobiletin acts anti-inflammatory on murine IL-10(-/-) colitis and human intestinal fibroblasts. Eur J Nutr. 2019;58(4):1391–1401. doi: 10.1007/s00394-018-1661-x.
[39] Sp N, Kang DY, Joung YH, et al. Nobiletin inhibits angiogenesis by regulating Src/FAK/STAT3-mediated signaling through PXN in ER^+ breast cancer cells. Int J Mol Sci. 2017;18(5):935. doi: 10.3390/ijms18050935.
[40] Malik S, Bhatia J, Suchal K, et al. Nobiletin ameliorates cisplatin-induced acute kidney injury due to its antioxidant, anti-inflammatory and anti-apoptotic effects. Exp Toxicol Pathol. 2015;67(7-8):427–433. doi: 10.1016/j.etp.2015.04.008.
[41] Noguchi S, Atsumi H, Iwao Y, et al. Nobiletin: a citrus flavonoid displaying potent physiological activity. Acta Crystallogr C Struct Chem. 2016;72(Pt 2):124–127. doi: 10.1107/S2053229616000577.
[42] Güvenç M, Cellat M, Gökçek İ, et al. Nobiletin attenuates acetaminophen-induced hepatorenal toxicity in rats. J Biochem Mol Toxicol. 2020;34(2):e22427. doi: 10.1002/jbt.22427.
[43] Zhao S, Liu Z, Wang M, et al. Anti-inflammatory effects of Zhishi and Zhiqiao revealed by network pharmacology integrated with molecular mechanism and metabolomics studies. Phytomedicine. 2018;50:61–72. doi: 10.1016/j.phymed.2018.09.184.
[44] Li H, Liu Z, Liu L, et al. Vascular protection of TPE-CA on hyperhomocysteinemia-induced vascular endothelial dysfunction through AA metabolism modulated CYPs pathway. Int J Biol Sci. 2019;15(10):2037–2050. doi: 10.7150/ijbs.35245.
[45] Liu L, Liu Z, Li H, et al. Naturally occurring TPE-CA maintains gut microbiota and bile acids homeostasis via FXR signaling modulation of the liver-gut axis. Front Pharmacol. 2020;11:12. doi: 10.3389/fphar.2020.00012.
[46] Henderson NC, Rieder F, Wynn TA. Fibrosis: from mechanisms to medicines. Nature. 2020;587(7835):555–566. doi: 10.1038/s41586-020-2938-9.
[47] Panizo S, Martínez-Arias L, Alonso-Montes C, et al. Fibrosis in chronic kidney disease: pathogenesis and consequences. Int J Mol Sci. 2021;22(1):408. doi: 10.3390/ijms22010408.
[48] Yang RY, Rabinovich GA, Liu FT. Galectins: structure, function and therapeutic potential. Expert Rev Mol Med. 2008;10:e17. doi: 10.1017/S1462399408000719.
[49] Pang X, Qiao J. Galectin-1 inhibits PDGF-BB-induced proliferation and migration of airway smooth muscle cells through the inactivation of PI3K/Akt signaling pathway. Biosci Rep. 2020;40(6):BSR20193899. doi: 10.1042/BSR20193899.